Plant Physiology and Biochemistry 93 (2015) 29–33

Contents lists available at ScienceDirect

Plant Physiology and Biochemistry

journal homepage: www.elsevier.com/locate/plaphy

Mutagenesis during plant responses to UVB radiation

M. Holá, R. Vágnerová, K.J. Angelis*

Institute of Experimental Botany AS CR, Na Karlovce 1, 160 00 Prague 6, Czech Republic

ARTICLE INFO

Article history:
Received 28 September 2014
Accepted 16 December 2014
Available online 17 December 2014

Keywords:
UV dimers
DNA repair
Error-prone bypass
Comet assay
APT mutagenesis

ABSTRACT

We tested an idea that induced mutagenesis due to unrepaired DNA lesions, here the UV photoproducts, underlies the impact of UVB irradiation on plant phenotype. For this purpose we used protonemal culture of the moss *Physcomitrella patens* with 50% of apical cells, which mimics actively growing tissue, the most vulnerable stage for the induction of mutations. We measured the UVB mutation rate of various moss lines with defects in DNA repair (*pplig4*, *ppku70*, *pprad50*, *ppmre11*), and in selected clones resistant to 2-Fluoroadenine, which were mutated in the adenosine phosphotrasferase gene (*APT*), we analysed induced mutations by sequencing. In parallel we followed DNA break repair and removal of cyclobutane pyrimidine dimers with a half-life $\tau = 4$ h 14 min determined by comet assay combined with UV dimer specific T4 endonuclease V. We show that UVB induces massive, sequence specific, error-prone bypass repair that is responsible for a high mutation rate owing to relatively slow, though error-free, removal of photoproducts by nucleotide excision repair (NER).

1. Introduction

The majority of UVB photoproducts, pyrimidine dimers (CPD) and pyrimidine(6–4)pyrimidinone dimers (6–4 PP), are removed in plants by blue light (320–450 nm) induced direct dimer reversal with photolyases specific for CPDs as well as 6–4 PP (Britt, 1995). Light repair is efficient and error free, nevertheless half-life of CPDs removal is about 1 h (Pang and Hays, 1991) and for complete elimination of 6-4PPs are needed at least 2 h (Waterworth et al., 2002; Chen et al., 1994), during which other mechanisms can take place. In contrast to photoreactivation, dark repair pathways do not directly reverse DNA damage, but instead replace the damaged DNA with new, undamaged nucleotides. There are recognized to be two possible mechanisms relying either on excision of dimers or on their tolerance by trans-lesion synthesis, of which replicative polymerases are also capable (Rabkin et al., 1983). CPDs and 6–4 PP are recognized and removed due to their "bulky" distortion of the DNA double helix by nucleotide excision repair (NER), a repair mechanism able to cope with a broad spectrum of DNA lesions that disturb the conformation of DNA, by error-free replacement of the DNA strand containing the lesion in a range of 2–4 helical turns (20–40 nucleotides) by a newly synthesized patch. Both photoreactivation and NER are error free, and so we asked which mechanism underlay the generally observed high mutagenic as well as severe carcinogenic risk caused by UV irradiation. The most relevant form of UV for the induction of biological effects is UVB, since UVC hardly penetrates the Earth's atmosphere. In the present research we used a recently-described approach employing regenerating one-day-old protonemal tissue of *Physcomitrella patens* (Hola et al., 2013) for complex analysis of UVB genotoxic stress in laboratory conditions by parallel study of DNA damage, its repair and its mutagenic consequences in wild type and *pplig4*, *pprad50*, *ppmre11*, *ppku70* mutants, to ascertain the nature of observed high rates of UV mutagenesis.

2. Materials and methods

Detailed description of Materials and Methods is in Appendix A.

2.1. Plant material

P. patens (Hedw.) B.S.G. "Gransden 2004"wild type and *pplig4*, *pprad50*, *ppmre11* were described previously (Hola et al., 2013; Kamisugi et al., 2012) along with cultivation and treatment conditions. The *ppku70* mutant in the canonical non-homologous DSB repair pathway (C-NHEJ) was generated and kindly provided by D.

Abbreviations: A/N, comet assay protocol with alkaline unwinding step; *APT*, adenine phosphotrasnferase; BER, base excision repair; CPD, cyclobutyl pyrimidine dimer; 2FA, 2-Fluoroadenin; NER, nucleotide excision repair; N/N, neutral comet assay; 6–4 PP, pyrimidine(6–4)pyrimidinone dimer; SSB, DNA single strand break; τ, half-life; T4EndoV, T4 Endonuclease V.

* Corresponding author.
E-mail address: karel.angelis@gmail.com (K.J. Angelis).

http://dx.doi.org/10.1016/j.plaphy.2014.12.013
0981-9428/

G. Schaefer, Neuchatel University, Switzerland.

2.2. UV and Bleomycin treatment

Laboratory broadband UVB irradiation was carried in a Hoefer UV crosslinker with the unwanted UVC fraction filtered out by a cellulose acetate sheet (Britt et al., 1993) overlaying samples and a crosslinker UV gauge (Figure A.2). Insertion of the sheet increased by about 20% the time needed for the crosslinker to achieve the set irradiation dose; e.g. from 40 to 50 s to deliver dose 3 kJ m^{-2}. To block light repair, irradiation and recovery cultivation were performed in dark and collection and freezing of samples under red light in a darkroom. In mutation experiments, samples were kept in the dark for 24 h after irradiation to allow induction of mutations.

Bleomedac inj. (Medac, Hamburg, Germany) was used for Bleomycin treatment as previously described (Hola et al., 2013).

All studies were performed with protonemata 1 day following homogenisation, having approximately 50% of actively dividing cells (Fig. A.1).

2.3. Detection of DNA lesions

DNA single strand breaks (SSBs) were detected by an A/N comet assay using neutral protocol with an alkaline unwinding step (Angelis et al., 1999; Menke et al., 2001; Olive and Banath, 2006). For specific detection of CPDs, T4 endonuclease V (T4EndoV) digestion step was included in the protocol after cell lysis. T4EndoV enzyme was prepared as a crude lysate from overexpressing bacteria (Collins, 2011; Valerie et al., 1985). Thirty minutes digestion of nuclear DNA of cells irradiated by 3 kJ m^{-2} with T4EndoV diluted 1:500 at room temperature generated app. 95% DNA fragmentation (Fig. A.3). Without T4EndoV treatment, the fraction of fragmented DNA in comet tails increased after irradiation only to 10% from 1 to 2 % of background value.

Comets on slides were stained with SYBR Gold (Molecular Probes/Invitrogen), viewed in epifluorescence with a Nikon Eclipse 800 microscope and captured and evaluated by the LUCIA Comet cytogenetic software (LIM Inc., Czech Republic).

2.4. Analysis of comet assay data

The fraction of fragmented DNA in comet tails (% T DNA) was used as a measure of DNA damage, nevertheless for an easy comparison of SSBs and CPDs repair kinetics, comet data are rather expressed as % of remaining damage, where damage after UV irradiation at $t = 0$ is set 100% for both lesions (Eq. (A.1)).

Data in this study were obtained in at least three independent experiments. Measurements of blind-labelled comet slides included 25 evaluated comets of four independent gel replicas in each experiment that totalled at least 300 comets analysed per experimental point. Time-course data were analysed for one-phase decay kinetics by Prism v.5 program (GrafPad Software Inc., USA).

2.5. Isolation and analysis of APT mutants

The dose 500 J m^{-2} was used to induce mutations in *APT*. After irradiation, samples were kept in darkness for 24 h to block light repair and generate mutations. Mutation rates were measured as the number of *APT* mutants that appeared as green foci of regenerating clones resistant to 2-Fluoroadenine (2FA). Treated protonemata were cultivated on plates with 8 μM 2FA and emerging foci were allowed to form colonies. Stable clones were then counted. Randomly selected clones were further propagated and their *APT* locus was PCR amplified and sequenced to identify the mutation(s) responsible for resistance. Details of mutant analysis are in Appendix Figure A.4 and Table A.1.

3. Results and discussion

3.1. Repair of UVB induced lesions

Repair of CPDs and 6-4PPs by excision NER pathway proceeds in four steps: Recognition of distorted DNA double helix by a “bulky” lesion, incision of the DNA strand on both sides of a lesion, filling the gap by DNA repair synthesis and religation of a newly synthesized patch.

DNA breaks formed during the incision step of dimer repair can be followed as SSBs by the A/N comet assay because they lead to fragmentation of nuclear DNA. Kinetics of formation and removal of SSBs during repair is plotted in Fig. 1 (open circles). Data are expressed as % of remaining damage, with damage after UV irradiation at $t = 0$ set to 100%. An increased number of SSBs due to NER is observed during period of approximately 6 h, with a peak at 1 h, when the number of breaks nearly doubles and is then followed by a gradual decrease, indicating saturation of repair capacity after 1 h and steady-state progression of repair afterwards. After 6 h the level of SSBs is the same as immediately after UV irradiation.

Removal of CPDs from nuclear DNA was followed after their conversion to SSBs by digestion of nuclei already embedded on comet slides with the CPD specific endonuclease T4EndoV prior to DNA unwinding and electrophoresis. T4EndoV has two associated enzyme activities: pyrimidine dimer glycosylase cleaving the glycosyl bond of the 5′-pyrimidine of CPD and AP-endonuclease cleaving the phosphodiester bond at a glycosylase-generated AP site. The kinetics of CPD removal in *P. patens* follows first order kinetics with an estimated half-life $\tau = 4$ h 14 min (Fig. 1, closed circles). As reported in *Arabidopsis*, CPD dark repair is several times slower than light repair and this might be true also in *P. patens* (Britt et al., 1993).

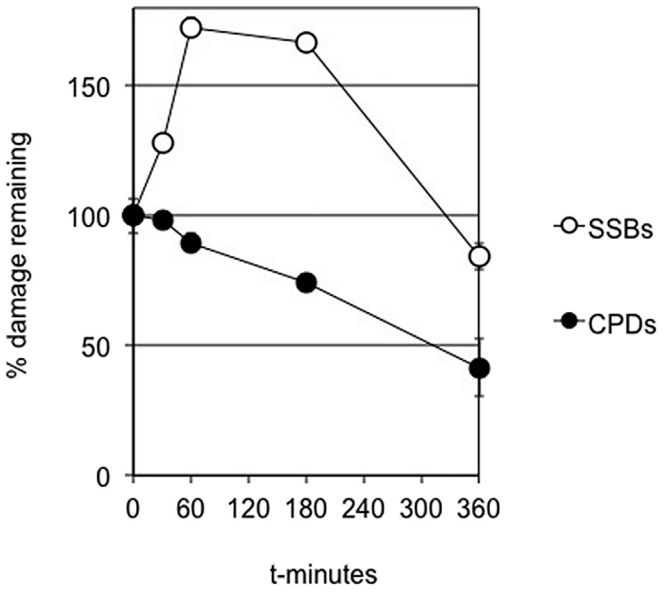

Fig. 1. The repair kinetics of SSBs and CPDs induced by 3 kJ m^{-2} UVB irradiation. Both SSBs and CPDs were determined in the same sample from which comet slides were prepared and processed either with or without the T4EndoV digestion step. Data are expressed as % of remaining damage, when damage after irradiation $t = 0$ is set to 100%. The number of SSBs first increases as a consequence of NER incisions, reaching a maximum after 1 h and then as NER proceeds their number decreases (opened circles). The number of induced CPDs gradually decreases from $t = 0$ following first order kinetics with a CPD half-life $\tau = 4$ h 14 min (closed circles).

3.2. UVB mutagenesis

Slow dark NER repair of UV dimers opens the possibility for their eventual, more rapid error-prone repair or any other error-prone tolerance mechanism that might underlie observed UV mutagenicity. For this reason we decided to detect mutagenesis endpoints as changes at the DNA sequence level.

Mutations in genes of nucleotide metabolism like *APT* confer resistance to halogenated bases like 2FA, which, when utilized by cell metabolism are toxic. This feature is used as a positive selection marker for identification of mutants. PCR amplification of the mutated gene DNA and its sequence analysis provides a description of the acquired mutations and gives an insight into how they occurred.

Firstly we examined the number of regenerating *APT* mutants in *P. patens* wild type and *pprad50*, *ppmre11*, *pplig4* and *ppku70* mutants, appearing spontaneously or induced by 500 J m^{-2} UVB, 1 mM MMS and 1 μg mL^{-1} Bleomycin and normalized the count to 1 g of dry tissue weight. Results are summarized in Fig. 2 (partial results of Bleomycin mutagenesis were previously published in (Hola et al., 2013; Kamisugi et al., 2012)). UV mutagenesis proved to be effective in the wt and repair mutants studied. Aside from an exceptional and enigmatic role of RAD50 in UV mutagenesis, we can speculate about the higher rate of UV mutagenesis in the *pplig4* background. Holá et al. (Hola et al., 2013) described a repair defect of oxidative damage by base excision repair (BER) and showed that LIG4, perhaps along with LIG1 (Waterworth et al., 2009) could substitute in plants that lacked LIG3 in this pathway. If we assume that absence of LIG4 abolishes the active error free BER pathway, then any error-prone repair or bypass of UV induced dimers becomes more relevant and could contribute to higher rates of mutagenesis. This is an interesting point, because BER repair of CPDs in plants was never previously seriously considered (Britt, 1995) regardless of the fact that this mechanism is active in bacteria (bacteriophage T4EndoV used in this study for detection of CPDs is an example) and perhaps also in other organisms.

3.3. Sequence analysis of UVB induced mutations

For detailed analysis of induced mutations we picked at random clones from mutation experiments and after their propagation isolated DNA and sequenced the *APT* locus. In all sequenced *APT* mutants we found mainly cytosine to thymine transitions (Table 1) that are typically formed after UV irradiation generating nearly exclusively pyrimidine dimers, but that rarely occur after other type of treatment like Bleomycin. UVB and Bleomycin induced mutations are summarized in Table B.1.

The production of mutations by agents that block DNA synthesis, such as CPDs, requires that there should be a mechanism to bypass the lesion so that the cell can remain viable even if the lesion is not removed. Trans-dimer bypass involves two steps: addition of a base opposite the damaged site and subsequent synthesis past the lesion. Error-prone bypass of CPD not compensated by removal of CPDs is responsible for a high mutation rate. The tendency to insert adenine opposite the first pyrimidine (and presumably also opposite the second) means that a large proportion of mutations will be "lost" because of insertion of the "correct" base, because thymine is the most frequent pyrimidine in dimers. Also, transitions should be more frequent than transversions because of the preference for purine insertions opposite pyrimidines (Rabkin et al., 1983). The high UV mutation rates indicate that in *P. patens* the error-prone bypass is very frequent and efficient on CPDs and on 6–4PPs that have not been removed by photolyases or by NER. This is also manifested by exclusive localization of UV induced transitions within exons 3, 4 and 5 in contrast to far more dispersed distribution of Bleomycin mutations (Fig. 3) that range from transitions/transversions, small (≧2 bp) deletions or insertions to large deletions up to 748 bp (Table B.1).

In our study we used artificial laboratory conditions (total dark or red light illumination) to dissect dark repair during dimer repair or 24-h fixation of mutations. Nevertheless in the real world under the daylight, when source of UV is sunshine, there is still approximately a 2-h window between induction of dimers by UV irradiation, before their elimination by light repair (Waterworth et al., 2002; Chen et al., 1994). NER is even slower than photoreactivation and thus cannot significantly contribute to offset consequences of quick error-prone repair. Moreover bypass is independent on the repair mechanism tested here by studying moss repair mutants and is solely dependent on ongoing DNA synthesis during irradiation. This is why we were able to follow the consequences of UV irradiation in a 1 day-subcultured protonemal culture with 50% of cells active in mitosis.

4. Summary

In actively dividing, apical plant cells, exposure to UVB induce

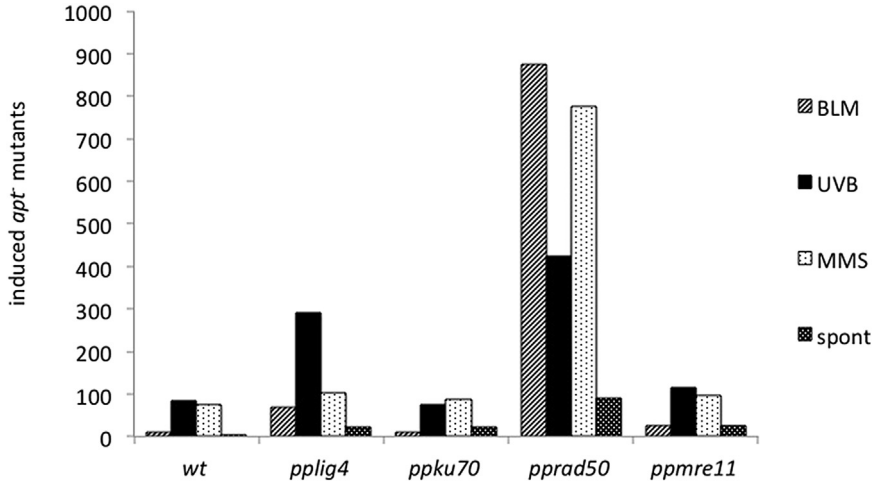

Fig. 2. Relative numbers of 2FA resistant mutants of *Physcomitrella patens* wild type and *pprad50*, *ppmre11*, *pplig4* and *ppku70*, differentiated into spontaneously appearing mutants and mutants induced by 500 J m^{-2} UVB, 1 mM MMS and 1 μg mL^{-1} Bleomycin respectively. The number of detected *APT* mutants is normalised to 1 g of dry tissue weight.

Table 1
Mutations induced by UVB irradiation within the *APT* locus of wt, *pprad50*, *ppmre11*, *pplig4* and *ppku70*. The observed spectra of induced mutations are principally base–substitution transitions.

Mutant line		Noncoding parts			Exons		
	APT mutant	Deletion	Insertion	Substitution	Deletion	Insertion	Substitution
WT	uvb3		**A**(3199)				T**C**CA → **T**(1369)
	uvb25			AG**G**T → **T**(2351)			
pprad50	uvb2						TT**G**A → **A**(1809)
	uvb23						T**C**CA → **TT**(1894)
	uvb29						AC**C**A → **T**(1650)
ppmre11	uvb3						G**C**TC → **T**(1813)
	uvb5						T**C**CA → **T**(1893)
pplig4	uvb4						T**C**CA → **T**(1369) CC**G**A → **A**(1576)
	uvb5						GC**C**A → **T**(1834)
	uvb20		**A**(643)				
ppku70	uvb1						T**C**CA → **TT**(1368)

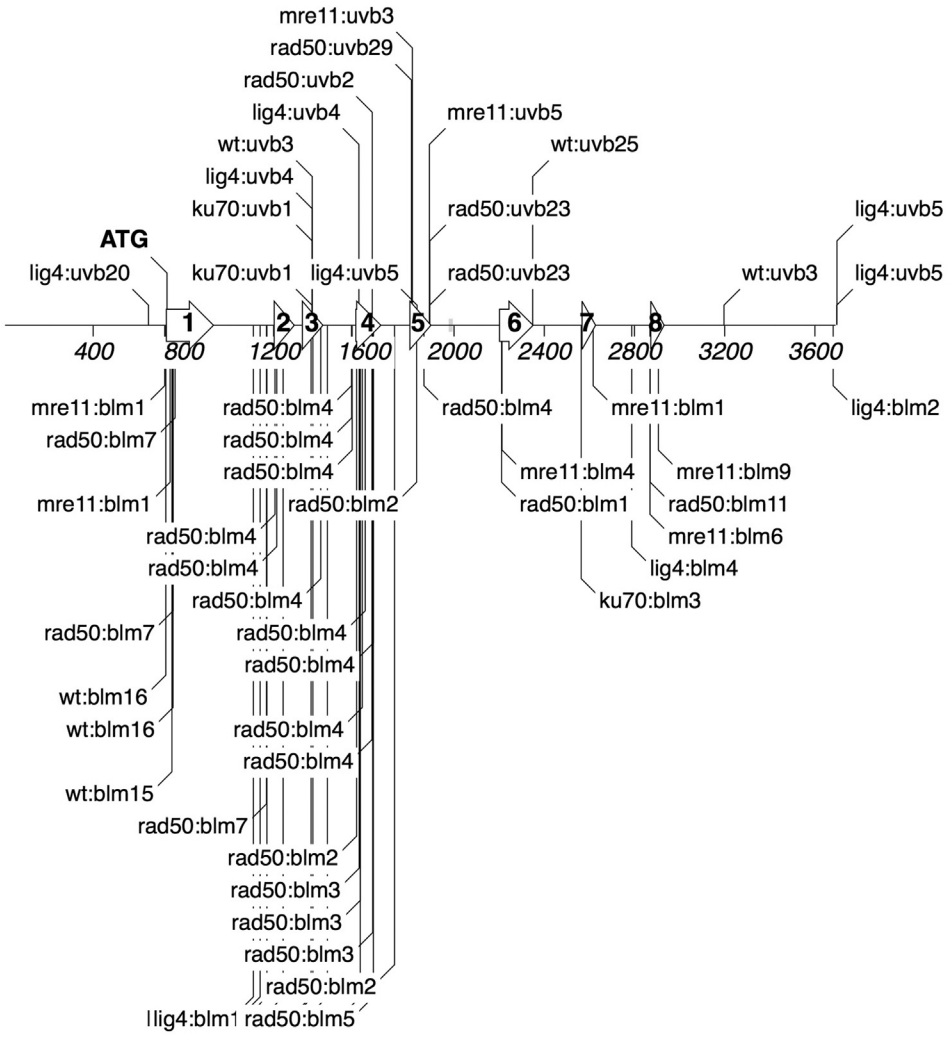

Fig. 3. Map of UVB and Bleomycin induced mutations within the *APT* locus. UVB induced mutations are depicted above and Bleomycin mutations below the schematic drawing of the *APT* locus, with ATG translation start indicated and exons represented as arrows. Mutation types for UVB are generally base substitutions, predominantly transitions in coding regions (Table 1 and Table B.1), whereas Bleomycin induces broad spectra of mutations from base substitutions of both types (transitions and transversions), insertions to deletions, in particular long deletions in *pprad50* and *ppmre11* (Table B.1).

robust mutagenesis via error-prone CPDs and 6-4PPs bypass DNA synthesis. Mutagenic activity is limited to DNA replication within dividing cells. When a mutated cell is not eliminated and mutation is tolerated during further plant development, then due to the clonal character of plant tissue it can initiate a change of phenotype (with or without external selection pressure). These changes do not need to be recognized as consequence of induced mutation, but rather considered as physiological effect of UVB. In this respect we proved the idea that induced mutagenesis due to unrepaired UV photoproducts could underlie the mechanism of UV impact on

plant phenotype.

Contributions

MH and RV performed *APT* mutation experiments, sequencing and mutation analysis. KJA did comet assay experiments, data evaluation and wrote the manuscript.

Acknowledgements

Supported by Czech Science Foundation (13-06595S) and Ministry of Education, Youth and Sport of CR (LD13006) grants.

Appendix A. Supplementary data

Supplementary data related to this article can be found at http://dx.doi.org/10.1016/j.plaphy.2014.12.013.

References

Angelis, K.J., Dusinska, M., Collins, A.R., 1999. Single cell gel electrophoresis: detection of DNA damage at different levels of sensitivity. Electrophoresis 20, 2133–2138.
Britt, A.B., 1995. Repair of DNA damage induced by ultraviolet radiation. Plant Physiol. 108, 891–896.
Britt, A.B., Chen, J.J., Wykoff, D., Mitchell, D., 1993. A UV-sensitive mutant of arabidopsis defective in the repair of pyrimidine-pyrimidinone(6-4) dimers. Science 261, 1571–1574.
Chen, J.J., Mitchell, D.L., Britt, A.B., 1994. A light-dependent pathway for the elimination of UV-induced pyrimidine (6-4) pyrimidinone photoproducts in arabidopsis. Plant Cell 6, 1311–1317.
Collins, A.R., 2011. The use of bacterial repair endonucleases in the comet assay. Methods Mol. Biol. 691, 137–147.
Hola, M., Kozak, J., Vagnerova, R., Angelis, K.J., 2013. Genotoxin induced mutagenesis in the model plant Physcomitrella patens. BioMed Res. Int. 2013, 535049.
Kamisugi, Y., Schaefer, D.G., Kozak, J., Charlot, F., Vrielynck, N., Hola, M., Angelis, K.J., Cuming, A.C., Nogue, F., 2012. MRE11 and RAD50, but not NBS1, are essential for gene targeting in the moss Physcomitrella patens. Nucleic Acids Res. 40, 3496–3510.
Menke, M., Chen, I., Angelis, K.J., Schubert, I., 2001. DNA damage and repair in Arabidopsis thaliana as measured by the comet assay after treatment with different classes of genotoxins. Mutat. Res. 493, 87–93.
Olive, P.L., Banath, J.P., 2006. The comet assay: a method to measure DNA damage in individual cells. Nat. Protoc. 1, 23–29.
Pang, Q., Hays, J.B., 1991. UV-b-inducible and temperature-sensitive photoreactivation of cyclobutane pyrimidine dimers in Arabidopsis thaliana. Plant Physiol. 95, 536–543.
Rabkin, S.D., Moore, P.D., Strauss, B.S., 1983. In vitro bypass of UV-induced lesions by Escherichia coli DNA polymerase I: specificity of nucleotide incorporation. Proc. Natl. Acad. Sci. U S A 80, 1541–1545.
Valerie, K., Henderson, E.E., de Riel, J.K., 1985. Expression of a cloned denV gene of bacteriophage T4 in Escherichia coli. Proc. Natl. Acad. Sci. U S A 82, 4763–4767.
Waterworth, W.M., Jiang, Q., West, C.E., Nikaido, M., Bray, C.M., 2002. Characterization of Arabidopsis photolyase enzymes and analysis of their role in protection from ultraviolet-B radiation. J. Exp. Bot. 53, 1005–1015.
Waterworth, W.M., Kozak, J., Provost, C.M., Bray, C.M., Angelis, K.J., West, C.E., 2009. DNA ligase 1 deficient plants display severe growth defects and delayed repair of both DNA single and double strand breaks. BMC Plant Biol. 9, 79.